Inorg. Chem. **2005**, *44*, 1922–1933

The Solution Structure of $[Cu(aq)]^{2+}$ and Its Implications for Rack-Induced Bonding in Blue Copper Protein Active Sites

Patrick Frank,*[,†,‡,§] Maurizio Benfatto,[†,∥] Robert K. Szilagyi,[†,⊥] Paola D'Angelo,[#] Stefano Della Longa,[¶] and Keith O. Hodgson[‡,§]

Department of Chemistry, Stanford University, Stanford, California 94305-5080, Stanford Synchrotron Radiation Laboratory, SLAC, Stanford University, Stanford, California 94309, Laboratori Nazionali di Frascati-INFN, Post Office Box 13, 00044 Frascati, Italy, Department of Chemistry and Biochemistry, Montana State University, Bozeman, Montana 59717, Dipartimento di Chimica, Università di Roma "La Sapienza", Piazzale Aldo Moro 5, 00185 Roma, Italy, and INFM, UdR Camerino, Italy, and Dipartimento di Medicina Sperimentale, Università L'Aquila, 67100 L'Aquila, Italy and Laboratori Nazionali di Frascati-INFN, Post Office Box 13, 00044 Frascati, Italy

Received April 28, 2004

The structure of $[Cu(aq)]^{2+}$ has been investigated by using full multiple-scattering theoretical (MXAN) analysis of the copper K-edge X-ray absorption (XAS) spectrum and density functional theory (DFT) to test both ideal T_d and square-planar four-coordinate, five-coordinate square-pyramidal, and six-coordinate octahedral $[Cu(aq)]^{2+}$models. The best fit was an elongated five-coordinate square pyramid with four Cu–O_{eq} bonds ($2\times$ 1.98 ± 0.03 Å and $2\times$ 1.95 ± 0.03 Å) and a long Cu–O_{ax} bond (2.35 ± 0.05 Å). The four equatorial ligands were D_{2d}-distorted from the mean equatorial plane by ±(17 ± 4)°, so that the overall symmetry of $[Cu(H_2O)_5]^{2+}$ is C_{2v}. The four-coordinate MXAN fit was nearly as good, but the water ligands ($4\times$ 1.96 ± 0.02 Å) migrated ±(13 ± 4)° from the mean equatorial plane, making the $[Cu(H_2O)_4]^{2+}$ model again D_{2d}-distorted. Spectroscopically calibrated DFT calculations were carried out on the C_{2v} elongate square-pyramidal and D_{2d}-distorted four-coordinate MXAN copper models, providing comparative electronic structures of the experimentally observed geometries. These calculations showed 0.85e spin on Cu^{II} and 0.03e electron spin on each of the four equatorial water oxygens. All covalent bonding was restricted to the equatorial plane. In the square-pyramidal model, the electrostatic Cu–O_{ax} bond was worth only 96.8 kJ mol^{-1}, compared to 304.6 kJ mol^{-1} for each Cu–O_{eq} bond. Both MXAN and DFT showed the potential well of the axial bond to be broad and flat, allowing large low-energy excursions. The irregular geometry and D_{2d}-distorted equatorial ligand set sustained by unconstrained $[Cu(H_2O)_5]^{2+}$ warrants caution in drawing conclusions regarding structural preferences from small molecule crystal structures and raises questions about the site-structural basis of the rack-induced bonding hypothesis of blue copper proteins. Further, previously neglected protein folding thermodynamic consequences of the rack-bonding hypothesis indicate an experimental disconfirmation.

Introduction

For about the last 40 years, aqueous, solution-state divalent copper ion, $[Cu(aq)]^{2+}$, has been primarily represented as the Jahn−Teller distorted octahedral hexaqua ion, $[Cu(H_2O)_6]^{2+}$,[1−4] although earlier it was presumed to have a tetragonal four-coordinate structure.[5,6] The transition in thinking between four- and six-coordinate $[Cu(aq)]^{2+}$ likely

* Author to whom correspondence should be addressed. Telephone: 1-650-723-2479. Fax: 1-650-723-4817. E-mail: frank@ssrl.slac.stanford.edu.
† These authors contributed equally to this work.
‡ Department of Chemistry, Stanford University.
§ Stanford Synchrotron Radiation Laboratory, SLAC, Stanford University.
∥ Laboratori Nazionali di Frascati-INFN.
⊥ Montana State University.
Università di Roma "La Sapienza".
¶ Università L'Aquila.

(1) Basolo, F.; Pearson, R. G. *Mechanisms of Inorganic Chemistry: A Study in Metal Complexes in Solution*, 2nd ed.; Wiley: New York, 1967.
(2) Cotton, F. A.; Wilkinson, G. *Basic Inorganic Chemistry*; John Wiley and Sons: New York, 1976.
(3) Cotton, F. A.; Wilkinson, G.; Murillo, C. A.; Bochman, M. *Advanced Inorganic Chemistry*, 6th ed.; Wiley-Interscience: New York, 1999.
(4) Wiberg, E.; Holleman, A. F. *Inoganic Chemistry*, 1st English ed.; Academic Press: San Diego, CA, 2001.

10.1021/ic0400639 CCC: $30.25 © 2005 American Chemical Society
Published on Web 02/22/2005

followed the important EPR experiments of Swift and Connick,[7] as well the results of single-crystal spectroscopy of hexaqua copper(II) complexes.[8]

However, Peisach and Mims later published the very relevant results of a linear electric field effect EPR study showing that $[Cu(aq)]^{2+}$ and other low molecular weight (MW) Cu^{II} complexes in aqueous solution do not have the centrosymmetry expected for a Jahn−Teller distorted octahedron but are D_{2d}-distorted.[9,10] This important result appears to have not found its way into descriptions of $[Cu(aq)]^{2+}$ in textbooks,[3,4,11] in the literature,[12−15] or in discussions of the geometric preferences of the Cu^{II} ion.[16−20]

A study of $[Cu(aq)]^{2+}$combining neutron diffraction and molecular dynamics indicated that this complex ion is a five-coordinate square pyramid.[21] However, the axially disposed fifth ligand could not be experimentally located more precisely than somewhere between 2 and 3.04 Å from the copper ion. This square-pyramidal geometry has since been disputed on the basis of copper K-edge extended X-ray absorption fine structure (EXAFS) experiments.[15] More recently, $[Cu(aq)]^{2+}$ was evaluated in terms of regular octahedral or square-pyramidal structures using the newly developed method, MXAN.[22−24] MXAN employs the full multiple-scattering approach to a description of the rising XAS K-edge and the first ∼200 eV of the EXAFS energy region and, with an initial structural model, extracts information about both the geometry and the bond metrics of the nearest neighbors of the absorbing atom.

This report describes an XAS and DFT investigation into the structure and stability of $[Cu(aq)]^{2+}$. MXAN fits are described that included geometrically unconstrained models allowing the four equatorial water ligands to migrate from the tetragonal plane and to rotate freely about the Cu−O axis during the fit. Four-, five-, and six-coordinate geometries were explored using MXAN analysis. The relative stabilities and electronic structures of the best-fit coordination geometries for $[Cu(aq)]^{2+}$ were then investigated and compared using density functional calculations. After this, the foundational assumption of rack-induced bonding in blue copper proteins[16,25,26] is herein evaluated in light of the geometric and bonding preferences of the unconstrained aqua Cu^{II} ion. Finally, the rack-bonding hypothesis itself is considered from perspectives of protein-folding thermodynamics that have thus far been neglected.

Materials and Methods

Sample Preparation and XAS Measurement. A 0.1 M Cu^{2+} aqueous solution was prepared by dissolving CuO in a slight excess of perchloric acid as described earlier.[23] X-ray absorption spectra at the Cu K-edge were recorded in transmission mode at the EMBL spectrometer at HASYLAB.[27] Measurements were performed at room temperature with a Si(220) double-crystal monochromator.

MXAN Fits. The XANES data analysis was performed with the MXAN code, using the same procedure previously described and published.[23] The X-ray absorption cross section was calculated in the framework of the full multiple-scattering scheme within the muffin-tin (MT) approximation for the shape of the potential with MT radii of 0.2 and 0.9 Å, for hydrogen and oxygen, respectively, and 1.2 Å for copper. The hydrogen MT radius chosen corresponded to about 0.06 electrons for the integral of the charge density. The real part of the exchange term was calculated using the Hedin−Lundqvist energy-dependent potential, while all of the inelastic losses were taken into account by a phenomenological method described in detail.[24]

A least-square fit of the experimental data in the space of the structural parameters was achieved using the MINUIT routine of the CERN library, which minimizes the R_{sq} function defined as

$$R_{sq} = n\sum_{i=1}^{m} w_i[(y_i^{th} - y_i^{exp})\epsilon_i^{-1}]^2 / \sum_{i=1}^{m} w_i$$

where n is the number of the independent structural parameters, m is the number of experimental data points, y_i^{th} and y_i^{exp} are the theoretical and experimental value of the absorption cross section, ϵ_i is the individual error in the experimental data set, and w_i is statistical weight. In our case, $w_i = 1$ and ϵ_i was constant and equal to 1% of the experimental jump. The MIGRAD subroutine of the MINUIT package calculates the statistical errors that are reported in Table 1. These errors stem from the correlation among refined parameters and are the only errors that can be calculated numerically. A previous investigation[28] on 3d metal ions in aqueous solution has shown that the overall error on the structural determination because of the approximations in the theory is normally within the statistical evaluation for such systems.

(5) Latimer, W. M.; Hildebrand, J. H. *Reference Book of Inorganic Chemistry*, 3rd ed.; Maxmillan: New York, 1951.
(6) Phillips, C. S. G.; Williams, R. J. P. *Inorganic Chemistry*; Oxford University: Oxford, U.K., 1966; Vol. 2.
(7) Swift, T. J.; Connick, R. E. *J. Chem. Phys.* **1962**, *37*, 307−320.
(8) Andreev, S. N.; Sapozhnikova, O. V. *Dokl. Akad. Nauk SSSR* **1964**, *156*, 855−857; CAN 61:58858.
(9) Peisach, J.; Mims, W. B. *Chem. Phys. Lett.* **1976**, *37*, 307−310.
(10) Peisach, J.; Mims, W. B. *Eur. J. Biochem.* **1978**, *84*, 207−214.
(11) Shriver, D. F.; Atkins, P.; H., L. C. *Inorganic Chemistry*; 2nd ed.; W. H. Freeman and Co.: New York, 1994.
(12) Beagley, B.; Eriksson, A.; Lindgren, J.; Persson, I.; Pettersson, L. G. M.; Sandström, M.; Wahlgren, U.; White, E. W. *J. Phys.: Condens. Matter* **1989**, *1*, 2395−2408.
(13) Salmon, P. S.; Neilson, G. W.; Enderby, J. E. *J. Phys. C: Solid State Phys.* **1988**, *21*, 1335−1349.
(14) Salmon, P. S.; Neilson, G. W. *J. Phys.: Condens. Matter* **1989**, *1*, 5291−5295.
(15) Persson, I.; Persson, P.; Sandström, M.; Ullström, A.-S. *J. Chem. Soc., Dalton Trans.* **2002**, 1256−1265.
(16) Malmström, B. G. *Eur. J. Biochem.* **1994**, *223*, 711−718.
(17) Williams, R. J. P. *Eur. J. Biochem.* **1995**, *234*, 363−381.
(18) Holm, R. H.; Kennepohl, P.; Solomon, E. I. *Chem. Rev.* **1996**, *96*, 2239−2314.
(19) Gray, H. B.; Malmström, B. G.; Williams, R. J. P. *J. Biol. Inorg. Chem.* **2000**, *5*, 551−559.
(20) Pranowo, H. D.; Rode, B. M. *Chem. Phys.* **2001**, *263*, 1−6.
(21) Pasquarello, A.; Petri, I.; Salmon, P. S.; Parisel, O.; Car, R.; Tóth, É.; Powell, D. H.; Fischer, H. E.; Helm, L.; Merbach, A. E. *Science* **2001**, *291*, 856−859.
(22) Benfatto, M.; Della Longa, S. *J. Synchrotron Radiat.* **2001**, *8*, 1087−1084.
(23) Benfatto, M.; D'Angelo, P.; Della Longa, S.; Pavel, N. V. *Phys. Rev. B: Condens. Matter Mater. Phys.* **2002**, *65*, 174205.
(24) Benfatto, M.; Della Longa, S.; Natoli, C. R. *J. Synchrotron Radiat.* **2003**, *10*, 51−57.
(25) Malmström, B. G. In *Oxidases and Related Redox systems*; King, T. E., Mason, H. S., Morrison, M., Eds.; Wiley: New York, 1965; Vol. 1.
(26) Vallee, B. L.; Williams, R. J. P. *Proc. Natl. Acad. Sci. U.S.A.* **1968**, *59*, 498−505.
(27) Hermes, C.; Gilberg, E.; Koch, M. H. J. *Nucl. Instrum. Methods Phys. Res.* **1984**, *222*, 207−214.
(28) D'Angelo, P.; Benfatto, M.; Della Longa, S.; Pavel, N. V. *Phys. Rev. B: Condens. Matter Mater. Phys.* **2002**, *66*, 064209.

Table 1. Structural (R and α), Core-Hole Lifetime (Γc), and Quality of Fit (R_{sq}) Parameters Derived from the MXAN Data Analysis

equatorial symmetry: D_{2d}[a]	R_{1eq} (Å)	R_{2eq} (Å)	R_{ax} (Å)	α (deg)	Γc (eV)[b]	R_{sq}
four coordinate	1.96 ± 0.02	1.96 ± 0.02		13 ± 4.0	1.94	2.07
five coordinate	1.98 ± 0.03	1.95 ± 0.03	2.35 ± 0.05	17 ± 4	1.77	1.32
six coordinate	1.99 ± 0.04	1.99 ± 0.04	2.63 ± 0.05	7 ± 12	2.05	3.1

[a] This designation refers to the symmetry of the tetragonal ligands only, neglecting the hydrogen atoms. The overall symmetry of the five- and six-coordinate complex ions, including hydrogens, is C_{2v}. The errors represent one standard deviation. [b] The core-hole lifetime width of copper is 1.55 eV.[45]

Electronic Structure Calculations. Spectroscopically calibrated, hybrid density functional calculations (B(38HF)P86) were performed using the Gaussian98[29] package on a 32-cpu SGI Origin 2000 supercomputer. The Becke88[30] exchange and Perdew86[31] correlation functionals were used with 38% of the total density functional exchange replaced with HF exchange giving an accurate bonding description as discussed for other cupric systems.[32] The triple-ζ (VTZ*)[33] and double-ζ (6-31G*)[34−36] Gaussian-type all-electron basis sets were employed in all calculations with polarization functions for the metal and ligands, respectively, which have been shown to be a converged basis set (BS5) for Cu^{II}-containing systems.[32,37,38] Atomic spin densities were calculated by means of Weinhold's Natural Population Analysis (NPA).[39−44] Because of the flat potential energy surface of the cupric complexes, geometry optimizations were carried out using Cartesian coordinates to achieve convergence. The stationary points were validated with frequency calculations to be shown as equilibrium geometries. Solvent effects, i.e., the secondary solvation shell, were implemented through the polarized continuum method (PCM).[42−44]

Results

MXAN Fits to the K-Edge XAS of $[Cu(aq)]^{2+}$. The MXAN approach to structure determination starts with the K-edge X-ray absorption (XAS) spectrum and calculates a best fit to data points using the full multiple-scattering formalism within the constraints of the chosen structural model.[22,24] The MXAN method is particularly sensitive to geometric factors because it takes specific account of the XAS edge region where multiple-scattering effects make large contributions to X-ray absorption spectra. The mean-free path of the photoelectron both in the XAS K-edge and the EXAFS energy region ranges from 2.2 to 6 Å depending on the energy and including core-hole lifetime and the experimental resolution.[22,24] Thus, MXAN fits to XAS spectra can recover both the distance metrics and the geometry around the absorbing atom, in principle, to regions beyond the first coordination shell. Inclusion of the first 50 eV of the K-edge XAS energy region in the fit also makes MXAN structure determinations less sensitive to thermal motion (Debye−Waller factors) than the usual EXAFS fits because the DW $\exp(-k^2\sigma^2)$ term becomes small at low k.[24] A previous MXAN study restricted to geometrically constrained $[Cu(aq)]^{2+}$ models gave as best fit a five-coordinate square-pyramidal model with four coplanar waters at 1.96(1) Å and one axial water at 2.39(6) Å.[23]

We report here a new MXAN analysis of the XAS spectrum of $[Cu(aq)]^{2+}$ that imposed no geometric constraints on the initial model. Migration of the water ligands from the equatorial plane and rotation of these ligands about the Cu−O axis were both allowed, as was variation in the Cu^{II}−O bond lengths. The aim was to refine the structure of $[Cu(aq)]^{2+}$ and to find the most stable geometry of unconstrained Cu^{II} aqua ion consistent with the copper K-edge XAS spectrum.

In the first step of the analysis, the compatibility of the XANES spectrum with the existence of a four-coordinate strictly tetrahedral geometry for $[Cu(aq)]^{2+}$ was assessed by performing a minimization of the experimental data while imposing T_d symmetry. In this fit, only the Cu^{II}−water ligand distances were allowed to vary. The results of the fitting procedure are shown in Figure 1a and correspond to an ideal tetrahedral configuration of waters around the Cu^{II} ion at a best fit distance of 1.96 Å. The agreement between the experiment and the calculated model is poor, especially in the low-energy range of the spectrum, and this is also evident from the high value of the error function, $R_{sq} = 9.97$.[23]

An octahedral model was then tested while allowing the equatorial waters to rotate and to move from the mean CuO_4 equatorial plane (angle α) in addition to allowing all of the Cu−OH_2 distances to vary. The best-fit calculated XANES spectrum is shown in Figure 1b and is in better agreement with the experimental data ($R_{sq} = 3.1$). The values of the fitted parameters are reported in Table 1. These results are similar to the MXAN best-fit XANES spectrum previously

(29) Frisch, M. J.; Trucks, G. W.; Schlegel, H. B.; Scuseria, G. E.; Robb, M. A.; Cheeseman, J. R.; Zakrzewski, V. G.; Montgomery, J. A., Jr.; Stratmann, R. E.; Burant, J. C.; Dapprich, S.; Millam, J. M.; Daniels, A. D.; Kudin, K. N.; Strain, M. C.; Farkas, O.; Tomasi, J.; Barone, V.; Cossi, M.; Cammi, R.; Mennucci, B.; Pomelli, C.; Adamo, C.; Clifford, S.; Ochterski, J.; Petersson, G. A.; Ayala, P. Y.; Cui, Q.; Morokuma, K.; Malick, D. K.; Rabuck, A. D.; Raghavachari, K.; Foresman, J. B.; Cioslowski, J.; Ortiz, J. V.; Stefanov, B. B.; Liu, G.; Liashenko, A.; Piskorz, P.; Komaromi, I.; Gomperts, R.; Martin, R. L.; Fox, D. J.; Keith, T.; Al-Laham, M. A.; Peng, C. Y.; Nanayakkara, A.; Gonzalez, C.; Challacombe, M.; Gill, P. M. W.; Johnson, B. G.; Chen, W.; Wong, M. W.; Andres, J. L.; Head-Gordon, M.; Replogle, E. S.; Pople, J. A. *Gaussian 98*, revision A.1; Gaussian, Inc.: Pittsburgh, PA, 1998.
(30) Becke, A. D. *Phys. Rev. A: Gen. Phys.* **1988**, *38*, 3098−3100.
(31) Perdew, J. P. *Phys. Rev. B: Condens. Matter Mater. Phys.* **1986**, *33*, 8822−8824.
(32) Szilagyi, R. K.; Metz, M.; Solomon, E. I. *J. Chem. Phys. A* **2002**, *106*, 2994−3007.
(33) Schäfer, A.; Horn, H.; Ahlrichs, R. *J. Chem. Phys.* **1992**, *97*, 2571−2577.
(34) Hariharan, P. C.; Pople, J. A. *Theor. Chim. Acta* **1973**, *28*, 213−222.
(35) Francl, M. M.; Pietro, W. J.; Hehre, W. J.; Binkley, J. S.; Gordon, M. S.; DeFrees, D. J.; Pople, J. A. *J. Chem. Phys.* **1982**, *77*, 3654−3665.
(36) Rassolov, V. A.; Pople, J. A.; Ratner, M. A.; Windus, T. L. *J. Chem. Phys.* **1998**, *109*, 1223−1229.
(37) Siegbahn, P. E. M.; Blomberg, M. R. A. *Chem. Rev.* **2000**, *100*, 421−437.
(38) Ryde, U.; Olsson, M. H. M.; Roos; O., B.; Borin, A. C. *Theor. Chem. Acc.* **2001**, *105*, 452−462.
(39) Foster, J. P.; Weinhold, F. *J. Am. Chem. Soc.* **1980**, *102*, 7211−7218.
(40) Reed, A. E.; Curtiss, L. A.; Weinhold, F. *Chem. Rev.* **1988**, *88*, 899−926.
(41) Carpenter, J. E.; Weinhold, F. *J. Mol. Struct.* **1988**, *169*, 41−62.
(42) Miertus, S.; Scrocco, E.; Tomasi, J. *Chem. Phys.* **1981**, *55*, 117−129.
(43) Tomasi, J.; Persico, M. *Chem. Rev.* **1994**, *94*, 2027−2094.
(44) Cossi, M.; Barone, V.; Cammi, R.; Tomasi, J. *Chem. Phys. Lett.* **1996**, *255*, 327−335.

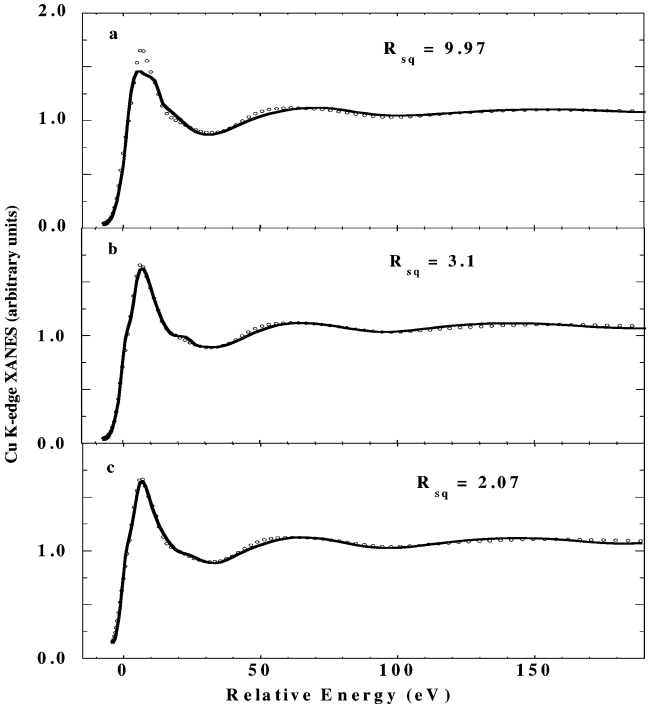

Figure 1. Copper K-edge spectra of [Cu(aq)]$^{2+}$ (○) and the MXAN fit to the XAS data (—). The data were fit with (a) a regular tetrahedral (T_d) model, (b) a six-coordinate axially elongated (D_{4h}) octahedron, and (c) a four-coordinate D_{2d} model. The latter two fits allowed the axial waters to excurse from the tetragonal plane. The R_{sq} is a measure of the goodness-of-fit (see the text).

obtained for an equatorially constrained Jahn−Teller distorted octahedron, which gave four oxygens at 1.99(1) Å and two axial oxygens at 2.56 Å (R_{sq} = 2.4).[23]

The increase in the value of R_{sq} for the unconstrained version of the two octahedral MXAN fits rests upon the use of four geometrical parameters instead of the three parameters of the equatorially constrained model.[23] The opening of a new degree of freedom does not significantly change the quality of the fit, in that the error function R_{sq} normalized to the number of geometrical parameters is almost equal in both cases and the metric results are not significantly different from the prior fit in which the water ligands were constrained to the equatorial plane. In either octahedral case, however, the axial Cu−O distance is much longer than the 2.36 Å[23] or 2.29 Å[15] determined by directly fitting the copper K-edge EXAFS spectrum of [Cu(aq)]$^{2+}$.

Additional possible structures were then evaluated starting from an unconstrained four-coordinate [Cu(aq)]$^{2+}$, where three structural parameters were refined, namely, two sets of Cu−O equatorial bond lengths and the α angle defining the deviation of the Cu−O axis from the tetragonal plane. Application of the MXAN method produced a best fit model with four waters surrounding the Cu^{II} ion at a distance of 1.96 Å in a D_{2d} arrangement. The correspondence between this fit and the data (R_{sq} = 2.07) proved significantly better than either fit using an octahedral six-coordinate model. The XANES theoretical curve and the experimental spectrum are compared in Figure 1c and the best-fit values for the full set of structural parameters are listed in row 1 of Table 1, together with the core-hole lifetime (Γc) at the copper K-edge

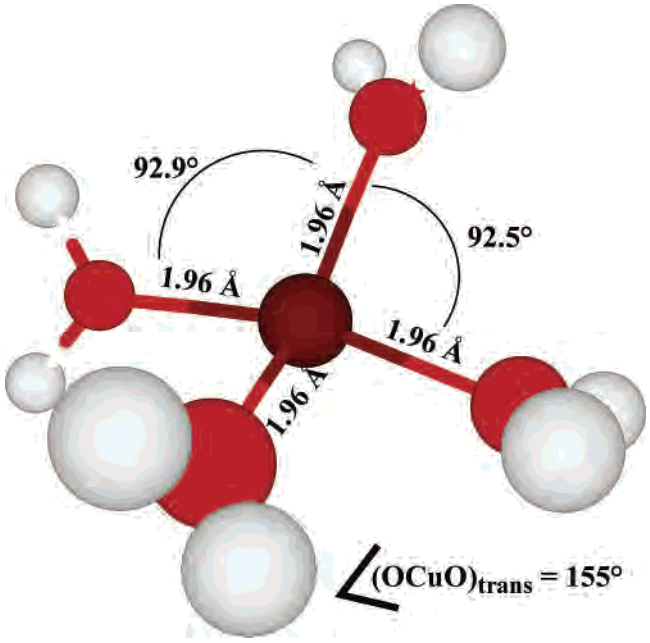

Figure 2. Structural representation of the best four-coordinate D_{2d} model for [Cu(aq)]$^{2+}$. All four Cu−O bond lengths are 1.96 Å, and the waters are ±13° from the mean equatorial plane (see Table 1).

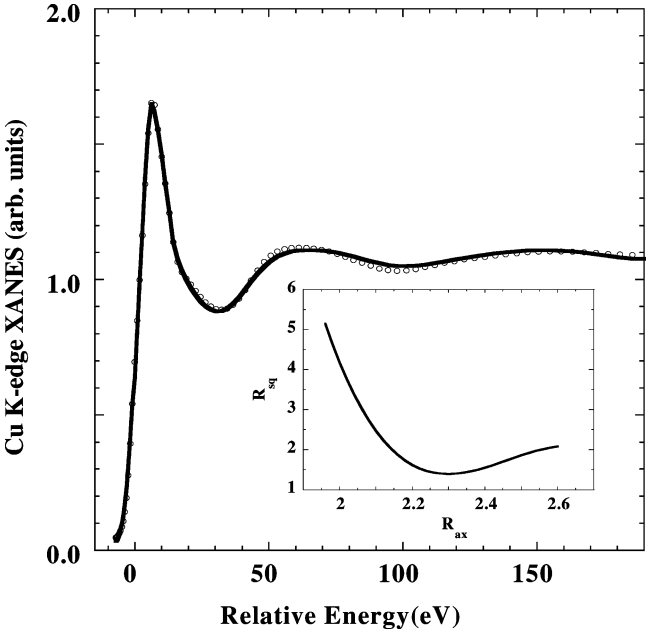

Figure 3. Copper K-edge spectra of [Cu(aq)]$^{2+}$ (○) and the MXAN fit to the XAS data (—) using an axially elongated square-pyramidal model. See Table 1 for the structural parameters. The inset plots goodness-of-fit (R_{sq}) versus axial bond-length (R_{ax}), showing the relatively broad and flat minimum for Cu−O_{ax}. See the text for discussion.

found by the program during the minimization. The structural output from this fit is shown in Figure 2.

The best representation of the structure and stability of [Cu(aq)]$^{2+}$ was obtained by performing a further MXAN analysis starting from a five-coordinate square pyramid and again allowing the four equatorial water ligands to migrate from the tetragonal plane and to rotate freely about the Cu−O axis. The best-fit analysis is shown in Figure 3, and the structural parameters obtained from the minimization correspond to a C_{2v} square-pyramidal structure, with the four

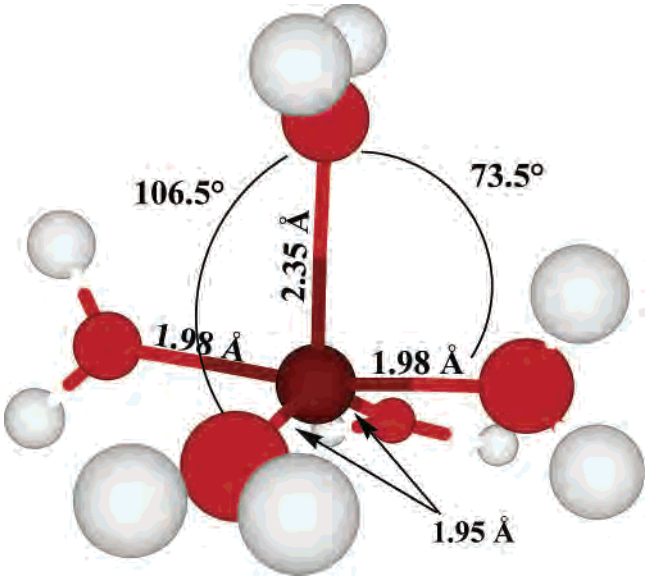

Figure 4. Structural representation of the best five-coordinate elongated square-pyramidal model for $[Cu(aq)]^{2+}$. The equatorial water ligands are displaced ±17° (see Table 1) from the mean equatorial plane and so are D_{2d} distorted.

equatorial waters noticeably D_{2d}-distorted ±(17±4)° from the equatorial plane and at a distance of 1.96(4) Å from Cu^{II}. The axial water ligand was found at 2.35(5) Å. All of the related geometrical information is reported in row 2 of Table 1. The structural model resulting from this fit is shown in Figure 4. The improved quality of the five-coordinate elongated square-pyramidal fit compared to the classical Jahn−Teller distorted six-coordinate model is shown by the significantly smaller value of the error function, R_{sq}, for the former fit (Table 1), as well as the closer correspondence of the value of the core-hole lifetime width (1.55 eV),[45] as calculated by MXAN during the fit. Indeed, taking into account the experimental resolution of 1.0 eV, the experimental line width of the Cu^{II} XAS spectrum is $\sqrt{[(1.55)^2 + (1.0)^2]} = 1.84$ eV, which is very close to the value found by MXAN for the five-coordinate model fit. Likewise, the (data − fit)^2 residuals showed that the fit using the five-coordinate model produced a significantly better match to the $[Cu(aq)]^{2+}$ XAS spectrum than did the J−T distorted six-coordinate octahedral model (Supplemental Figure 1 in the Supporting Information).

To assess the sensitivity of the XANES spectrum to the axial distance distribution, several MXAN minimizations were carried out on the five-coordinate model using fixed $Cu-O_{ax}$ distances and refining the other structural parameters. The results of this analysis are shown in the inset of Figure 3, where the R_{sq} values are plotted against the $Cu-O_{ax}$ distances. The picture that emerges is quite informative, because a reasonably good agreement between the experimental and theoretical curves (those with R_{sq} values lower than 2) is obtained over a wide range of $Cu-O_{ax}$ distances. Thus, this MXAN analysis suggests that models having elongated, weakly constrained axial copper−water bonds are preferred. The same finding was also obtained from analysis of the EXAFS region of the spectrum.[15,23] At large $Cu-O_{ax}$ distances, the error curve in the inset of Figure 3 approaches the value $R_{sq} = 2.07$, as found for the D_{2d}-distorted four-coordinate fit shown in Figure 1c and row 1 of Table 1.

Even though the present MXAN analysis shows the preference of $[Cu(aq)]^{2+}$ for an equatorial D_{2d}-distorted elongated square-pyramidal geometry, it is worth noting that the four-coordinate D_{2d} model produced a fit to the XANES spectrum that is in reasonable agreement with the experimental data. In both cases, the Γc values obtained from the MXAN analysis are consistent with the core-hole width of the Cu K-edge (Table 1).

Table 2. DFT Calculated Spin Densities for Two Structural Models of $[Cu(aq)]^{2+}$

atom type CN4	spin population	atom type CN5	spin population
Cu	0.839	Cu	0.852
$O1_{eq}$	0.037	$O1_{eq}$	0.030
$O2_{eq}$	0.037	$O2_{eq}$	0.031
$O3_{eq}$	0.037	$O3_{eq}$	0.036
$O4_{eq}$	0.037	$O4_{eq}$	0.037
H1	0.002	$O5_{ax}$	0.001
H1′	0.001	H1	0.001
H2	0.001	H1′	0.002
H2′	0.002	H2	0.002
H3	0.002	H2′	0.002
H3′	0.001	H3	0.002
H4	0.001	H3′	0.002
H4′	0.002	H4	0.002
		H4′	0.002
		H5	0.000
		H5′	0.000

Density Functional Investigation of the $[Cu(H_2O)_4]^{2+}$ and $[Cu(H_2O)_5]^{2+}$ Complexes. DFT calculations were used to comparatively explore the ground-state electronic structures and potential energy surfaces of D_{2d}-distorted $[Cu(H_2O)_4]^{2+}$ and axially elongated square-pyramidal C_{2v} $[Cu(H_2O)_5]^{2+}$. The structures of these complexes as deduced from the MXAN fits (Figures 2 and 4) were used as the starting geometries. When the energies corresponding to the best-fit geometries were calculated and compared to the energies of the optimized ligand and Cu^{2+} ion separately, the total metal−ligand binding energies were determined. These calculations gave 1218.0 kJ mol^{-1} for the four- and 1314.8 kJ mol^{-1} for the five-coordinate complexes (averages of 304.5 and 263.0 kJ mol^{-1} per Cu−O bond, respectively).

By analyzing the total atomic spin densities (Table 2), which can be taken as a measure of covalent delocalization of the single d-electron hole from the Cu^{II} onto the ligand, we found that in the four-coordinate case about 0.16 electron is equally distributed from the Cu onto the water ligands (Cu spin density 0.84e). In the case of the five-coordinate complex the covalent delocalization is the same (0.15e); however, it is only localized onto the four equatorial Cu−O bonds. The total atomic spin density, hence the covalency, of the axial ligand is less than 0.001e. Calculation of the binding energy of the water ligands relative to the four-coordinate complex gave only 96.8 kJ mol^{-1} for the axial Cu−O bond and 304.6 kJ mol^{-1} for each equatorial Cu−O bond. Thus, covalent bonding is restricted to the equatorial ligands of Cu^{II} (worth about 300 kJ mol^{-1} each), while the

(45) Krause, M. O.; Oliver, H. H. *J. Phys. Chem. Ref. Data* **1979**, *8*, 329−338.

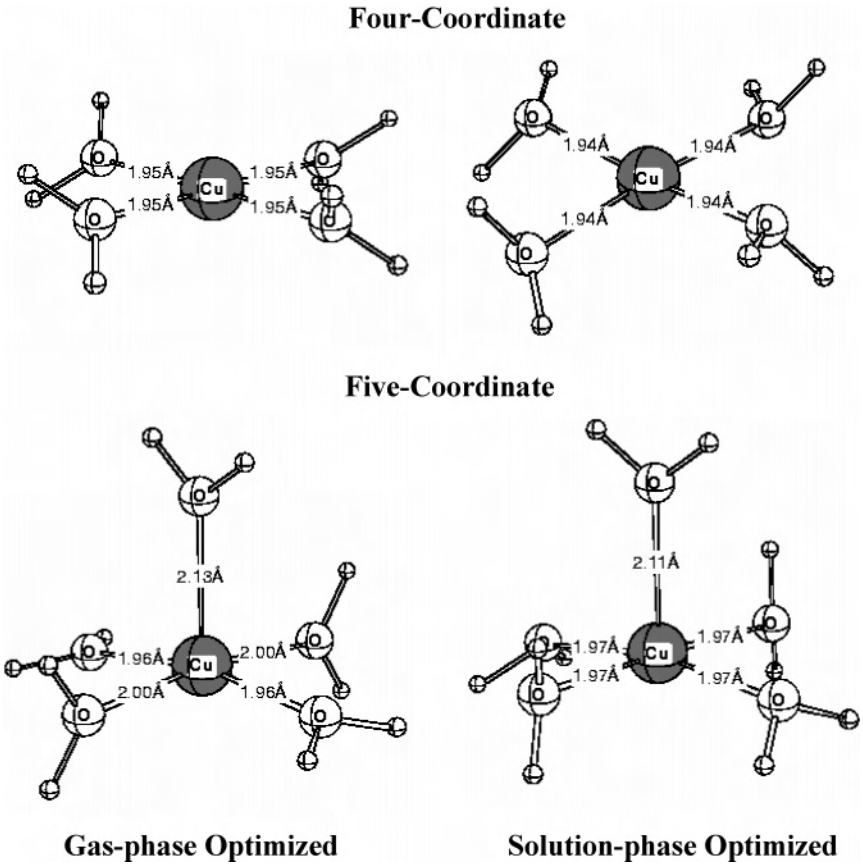

Figure 5. Molecular structures used in computations (Cartesian coordinates are given in the Supporting Information) starting from the initial MXAN fits of Figures 2 and 4 and showing the gas-phase optimized structures (column 1) and the solution-phase optimized structures (column 2). (Top) Four-coordinate models. (Bottom) Five-coordinate models.

axial ligand is bound by weak electrostatic interactions (worth about 100 kJ mol^{-1}) and does not significantly influence the bonding in the equatorial plane.

Optimization without the outer solvation shell (column 1 of Figure 5) lowers the energy of the four-coordinate complex by only 9.6 kJ mol^{-1}. This small energy difference corresponds to small changes in Cu−O bond lengths (0.01 Å); however, the D_{2d} distortion of the starting model is completely eliminated. This more than 12° angular change corresponds to only 8.4 kJ mol^{-1} and could take place easily in solution considering a b_{2u}-type distortion with a low force constant. It is worth noting in comparison with $[CuCl_4]^{2-}$ that, because of the large ligand−ligand repulsion, the D_{4h} tetragonal structure is a transition state between two D_{2d} structures as the Cl^-, Cl^- repulsive, and Cl^- and Cu^{2+} attractive interactions become optimized.[32] In the case of the neutral water ligands, the ligand−ligand repulsion is less than that for the anionic chloride ligands. The Cu atomic spin density ($0.82e^-$) in the optimized structure is very similar to that of the initial structure, and the covalency of the Cu−OH_2 bond is practically unchanged ($\Delta = 0.01e$).

Upon optimization of the five-coordinate complex, the largest change from the starting MXAN structure is in the axial O−Cu bond, which decreases from 2.35 Å to 2.13 Å. In the equatorial plane, the Cu−O bonds became asymmetrical as the pair of O_{ax}−Cu−O_{eq} angles associated with the longer Cu−O_{eq} bonds increase from 85.3° to 95.1°, while the other pair remains unchanged. These relatively large structural changes give a modest 73.7 kJ mol^{-1} energy lowering relative to the MXAN fit geometry. The overall geometry remains five-coordinate, and the structure continues to resemble the square pyramid as found for the MXAN fit, rather than trigonal-bipyramidal coordination. These coordination geometries involve different splittings of the Cu d orbitals, each of which would eliminate the Jahn−Teller distortion force. However, all optimizations starting from trigonal bipyramidal geometry led to the square-pyramidal geometry. Similar to the four-coordinate structures, the atomic spin densities of $[Cu(H_2O)_5]^{2+}$ do not change significantly during the optimization, and the axial water ligand does not contribute to the covalent bonding. The binding energy of the axial ligand in the fully optimized structures is 99.3 kJ mol^{-1}, which is practically identical to the axial bond strength in the MXAN fit structures ($\Delta =$ 2.5 kJ mol^{-1}), despite the ∼0.2 Å difference in bond lengths. This also indicates the flatness at the potential well minimum, and the electrostatic nature of the axial ligand interaction, in which the axial Cu−O bond length can undergo relatively large excursions at the expense of a small energy difference. Thus, the DFT calculation theoretically corroborates the MXAN fit result concerning this bond.

Optimization with the solvation shell modeled by PCM (column 2 of Figure 5) only slightly adjusts the Cu−O bond lengths, and the energy stabilization because optimization is negligible for the four-coordinate complex (2.5 kJ mol^{-1}) and small for the five-coordinate complex (19.3 kJ mol^{-1}).

The only significant difference between the gas-phase and the solution-phase structures is that the H atoms of the water ligands undergo out-of-plane distortion as the dipoles from the surrounding continuum compete with the Cu^{II} ion for the water ligands.

Overall, the density functional calculations reveal a flat potential energy surface around the Cu^{2+} ion with water coordination. The large structural changes within small energy differences suggest a highly dynamic picture of the bonding in the solvated Cu^{II} ion. The axial Cu−O distance and the out-of-plane angles of the equatorial ligands can vary easily giving an average molecular structure of five-coordinated Cu^{II} with D_{2d}-distorted equatorial ligands as determined from the XAS experiment. It is worth noting that, in terms of the overall molecular geometry, the DFT optimizations agree with the MXAN fits in favoring the five-coordinate structure over the four-coordinate structure.

Discussion

Solution Structure of $[Cu(aq)]^{2+}$. The above results extend previous EXAFS,[15,23] neutron diffraction,[21] and large-angle X-ray scattering (LAXS) studies[15] that in sum examined a series of structures for $[Cu(aq)]^{2+}$ beyond the six-coordinate Jahn−Teller elongated octahedron and five-coordinate axially elongated square pyramid. The EXAFS studies in particular were almost indistinguishable in outcome, producing the same bond metrics and eliminating the regular square-pyramidal and trigonal-bipyramidal models for $[Cu(aq)]^{2+}$. The LAXS/EXAFS study concluded in favor of the Jahn−Teller axially elongated six-coordinate model based on a perception of better Debye−Waller values. However, the known correlation between the coordination number and Debye−Waller value, and the finding that the relative magnitudes of the axial and equatorial Debye−Waller values for the five- and six-coordinate models were the same within error make this choice less than definitive.

Within the constraints of an MXAN fit, a difference of 20−30% in R_{sq} error is insufficient to allow a clear distinction between competing models. The R_{sq} values distinguishing the D_{2d}-distorted four-coordinate model ($R_{sq} = 2.07$) and the equatorial D_{2d}-distorted square-pyramidal model ($R_{sq} = 1.32$) are outside this range but are less than the ∼100% change in R_{sq} that would sustain a completely unambiguous choice between them. However, the previous fits to EXAFS data did unambiguously eliminate any four-coordinate model for $[Cu(aq)]^{2+}$ and favored but could not clearly distinguish between five and six coordination.[15,23] The MXAN study reported here clearly eliminated the competing six-coordinate Jahn−Teller octahedral model for $[Cu(aq)]^{2+}$ based on the >200% drop in R_{sq} (Table 1) and the significant decrease in unfit residuals (Supplemental Figure 1 in the Supporting Information) produced by the elongated D_{2d}-distorted square-pyramidal model.

Therefore, the combined MXAN and EXAFS results unambiguously show that in water solution, in which neither ligand number nor ligation geometry are constrained, the Cu^{II} ion assumes a C_{2v} five-coordinate axially elongated square pyramid in which the four tightly bound equatorial waters are on average staggered 17° above or below the mean CuO_4 equatorial plane in a D_{2d}-like arrangement. This finding corroborates the square-pyramidal coordination detected using neutron diffraction and molecular dynamics calculations[21] but now with a precise measure of the $Cu^{II}-O_{ax}$ distance and the new structural element of equatorial D_{2d} distortion.

The DFT study further revealed that only the equatorial water ligands participate in covalent bonding with the singly occupied $3d_{x^2-y^2}$ orbital of Cu^{II}. The small difference (50 kJ mol^{-1}) in the average Cu−O bond energy between D_{2d}-distorted $[Cu(H_2O)_4]^{2+}$ and C_{2v} $[Cu(H_2O)_5]^{2+}$ is primarily due to electrostatic bonding by the axial water ligand. The weakly bound axial water and the flat potential minimum of this bond should readily permit large amplitude excursions from the axial equilibrium distance. Geometry optimizations on the four-coordinate MXAN model indicated that, on elongation of the weak axial copper−water bond or on dissociation of the axial water ligand, the D_{2d} distortion of the four equatorial waters most likely decreases by 12° at most, at an expense of about 8 kJ mol^{-1}. Upon coordination of the axial water ligand, Cu^{II} can adopt the five-coordinate geometry at the expense of a similarly small reorganization energy. These considerations imply a dynamical "breathing mode" picture of $[Cu(H_2O)_5]^{2+}$ that includes rather large amplitude vibrations of the axial water ligand accompanied by D_{2d} wagging of the equatorial waters. D_{2d}-distorted $[Cu(H_2O)_4]^{2+}$ can have a transitory physical existence in ligand exchange of solvent water with bound water in $[Cu(H_2O)_5]^{2+}$ by a dissociative mechanism involving cleavage of the $Cu^{II}-O_{ax}$ bond.[46]

The comparatively small energy difference between D_{2d}-distorted four-coordinate $[Cu(H_2O)_4]^{2+}$ and equatorially D_{2d}-distorted five-coordinate $[Cu(H_2O)_5]^{2+}$ implies that the relative stability of these conformations may be altered by a coordination environment, e.g., in biological systems, that may lower the already small energy difference between four- and five-coordinate structures. For example, Cu3(a) within the T3 active site of T_2D laccase exhibits an approximately 1:1 partition between an irregular $[Cu(His)_4(H_2O)]^{2+}$ square pyramid and a distorted $[Cu(His)_3(H_2O)]^{2+}$ tetrahedron.[47] Alternatively, the temperature-dependent EPR spectrum of [bis(*N*,*N*-dimethyl-L-α-isoleucinato)Cu^{II}] indicates a square-pyramidal five-coordinate complex below 300 K in deuterated methanol, transitioning to an equatorially distorted four-coordinate Cu^{II} with the loss of the axial ligand above this temperature.[48,49] This transition is particularly illustrative because the axial ligand is lost in favor of weak van der Waals interactions that can occur between the trans-eclipsed hydrocarbon side chains of the two isoleucinato ligands. These examples reflect the relative weakness of the axial

(46) Åkesson, R.; Pettersson, L. G. M.; Sandström, M.; Wahlgred, U. *J. Am. Chem. Soc.* **1994**, *116*, 8705−8713.
(47) Ducros, V.; Brzozowski, A. M.; Wilson, K. S.; Østergaard, P.; Schneider, P.; Svendson, A.; Davies, G. J. *Acta Crystallogr., Sect. D* **2001**, *57*, 333−336.
(48) Noethig-Laslo, V.; Paulic, N.; Basosi, R.; Pogni, R. *Polyhedron* **2002**, *21*, 1643−1649.
(49) Sabolović, J.; Noethig-Laslo, V. *Cell. Mol. Biol. Lett.* **2002**, *7*, 151−153.

Cu^{II}−ligand bond, and the ease with which a four-coordinate complex can become the structural energy minimum.

The question of the slow self-exchange rate [50,51] for $[Cu(aq)]^{2+}/[Cu(aq)]^{+}$ is not necessarily exacerbated by the finding that in water solution Cu^{II} exists within a D_{2d}-distorted elongate square pyramid (we thank an anonymous reviewer for bringing this issue to our attention). The structure of $[Cu(aq)]^{+}$, often presumed to be the tetrahedral tetraaqua ion, $[Cu(H_2O)_4]^{+}$,[51] is in fact unknown and may be a weakly bound[52] linear diaqua ion, $[Cu(H_2O)_2]^{+}$, in analogy with $[Cu(NH_3)_2]^{+}$.[53−55] In this case, reduction of $[Cu(H_2O)_5]^{2+}$ would be accompanied by very large structural changes and thus a large reorganization energy, accounting for the slow self-exchange rate.

The Implications of D_{2d}-Distorted $[Cu(H_2O)_5]^{2+}$ for Rack-Induced Bonding in Blue Copper Proteins. The preference of unconstrained $[Cu(aq)]^{2+}$ for noncentrosymmetric ligation and equatorial D_{2d} distortion invites a re-evaluation of the inorganic structural foundation for the rack-bonding theory as applied to blue copper protein sites.

The original rack-bonding hypothesis of blue copper protein sites is that blue copper proteins rigidly force Cu^{II} to depart from a preferred equatorial D_{4h} ligand geometry.[16,17,19,25,26,56] This original rack hypothesis was explicitly based on the crystal structures of relatively low MW Cu^{II} complexes in which the Jahn−Teller distorted octahedron is standard and the equatorial ligands are preferentially D_{4h}.[16,19,26] The reference complexes on which this hypothesis depended included the crystalline all-oxygen liganded equatorial D_{4h} aquated complex $CuSO_4{\cdot}5H_2O$,[26] in which the unconstrained structural preferences of Cu^{II} are likely to be similar to that of D_{2d}-distorted $[Cu(H_2O)_5]^{2+}$. The equatorial planarity of crystalline Cu^{II} complexes was later contrasted with the trigonally distorted tetrahedral arrangement of the ligand suite in the blue copper protein site. The former was represented as preferred, and the latter was represented as energetically disfavored and imposed by the protein fold. The excess energy of the nonoptimal Cu^{II} site, responsible for the strain resisted by the protein rack, was estimated to be worth ∼70 kJ mol^{-1}.[16]

An alternative rack-induced bonding hypothesis has more recently assigned the nonoptimal geometry to the reduced Cu^{I} site[57−62] and placed the strain in an enforced elongate $Cu^{I}-S_{Met}$ bond rather than in the distorted tetrahedral geometry of the Cu^{II} site. This reformulation estimated a reduced rack strain of ∼29 kJ mol^{-1}.[60−62] Both formulations of the rack hypothesis are currently defended in the literature and are discussed below.

In contrast to the rack-bonding premise, however, the evidence presented herein shows that, in water solution, $[Cu(H_2O)_5]^{2+}$ prefers D_{2d}-distorted equatorial ligands and that fully four-coordinate D_{2d}-distorted bonding is energetically accessible. Likewise, the LEFE EPR results of Peisach and Mims showed that a number of Cu^{II} complexes, such as $[Cu(aq)]^{2+}$ and $[Cu[ImH)_4]^{2+}$, and including CuN_2S_2 complexes (e.g., [bis(butyraldehyde thiosemicarbazide)Cu^{II}]) that more closely approximate the copper−sulfur covalence of the blue copper protein site,[63,64] all spontaneously adopt equatorial D_{2d} distortion when unconstrained in solution. Thus, the strict D_{4h} equatorial symmetry found to predominate in the crystal structures of low MW Cu^{II} complexes [19,65] appears to reflect crystal-packing forces superimposed upon metal−ligand bonding and ligand−ligand repulsion, because equatorial D_{2d} ligation is apparently a general structural preference of dissolved unconstrained Cu^{II} complexes. Therefore, the foundational premise of rack-induced bonding in blue copper proteins, namely, the fact that Cu^{II} has a strong preference for D_{4h}-symmetry equatorial ligands, is removed.

In addition to the new results reported here and the above discussion, support for the structural flexibility of Cu^{II} is found in the equatorial-binding symmetry provided by a dissolved peptide model of the plastocyanin active site, which apparently switches from planar to tetrahedrally distorted when the dielectric of the medium is reduced.[66] Four-coordinate $\{(n\text{-}C_4H_9)_4N)\}_2[Cu^{II}(o\text{-carborane})_2]$ is also significantly D_{2d}-distorted despite the ability of this chelating ligand to achieve near equatorial planarity in a similar crystalline environment, e.g., in $\{(n\text{-}C_4H_9)_4N)\}_2[Ni^{II}(o\text{-carborane})_2]$.[67]

A further consideration typically but not always[68] over looked is that the oxidized blue copper site *does not contain Cu^{II}*, because the valence hole of the oxidized site is thoroughly dispersed into a delocalized molecular orbital that includes a major cysteine sulfur ligand component.[69,70] The

(50) Flanagan, S.; Dong, J.; Haller, K.; Wang, S.; Scheidt, W. R.; Scott, R. A.; Webb, T. R.; Stanbury, D. M.; Wilson, L. J. *J. Am. Chem. Soc.* **1997**, *119*, 8857−8868.
(51) Rorabacher, D. B. *Chem. Rev.* **2004**, *104*, 651−697.
(52) Naskar, J. P.; Chowdhury, S.; Drew, M. G. B.; Datta, D. *New J. Chem.* **2002**, *26*, 170−175.
(53) Burnier, R. C.; Carlin, T. J.; Reents, W. D.; Cody, R. B.; Lengel, R. K.; Freiser, B. S. *J. Am. Chem. Soc.* **1979**, *101*, 7127−7129.
(54) Magnera, T. F.; David, D. E.; Stulik, D.; Orth, R. G.; Jonkman, H. T.; Michl, J. *J. Am. Chem. Soc.* **1989**, *111*, 5036−5043.
(55) Blumberger, J.; Bernasconi, L.; Tavernelli, I.; Vuilleumier, R.; Sprik, M. *J. Am. Chem. Soc.* **2004**, *126*, 3928−3938.
(56) Machezynski, M. C.; Gray, H. B.; Richards, J. H. *J. Inorg. Biochem.* **2002**, *88*, 375−380.
(57) Guckert, J. A.; Lowery, M. D.; Solomon, E. I. *J. Am. Chem. Soc.* **1995**, *117*, 2817−2844.
(58) Solomon, E. I.; LaCroix, L. B.; Randall, D. W. *Pure Appl. Chem.* **1998**, *70*, 799−808.
(59) Randall, D. W.; Gamelin, D. R.; LaCroix, L. B.; Solomon, E. I. *J. Biol. Inorg. Chem.* **2000**, *6*, 16−19.
(60) Szilagyi, R. K.; Solomon, E. I. *Curr. Opin. Chem. Biol.* **2002**, *6*, 250−258.
(61) DeBeer George, S.; Basumallick, L.; Szilagyi, R. K.; Randall, D. W.; Hill, M. G.; Nersissian, A. M.; Valentine, J. S.; Hedman, B.; Hodgson, K. O.; Solomon, E. I. *J. Am. Chem. Soc.* **2003**, *125*, 11314−11328.
(62) Solomon, E. I.; Szilagyi, R. K.; DeBeer George, S.; Basumallick, L. *Chem. Rev.* **2004**, *104*, in press.
(63) Holm, R. H.; Balch, A. L.; Davison, A.; Maki, A. H.; Berry, T. E. *J. Am. Chem. Soc.* **1967**, *89*, 2866−2874.
(64) Campbell, M. J. M.; Collis, A. J.; Grzeskowiak, R. *Bioinorg. Chem.* **1976**, *6*, 305−311.
(65) Raithby, P. R.; Shields, G. P.; Allen, F. H.; Motherwell, W. D. S. *Acta Crystallogr., Sect. B* **1999**, *56*, 444−454.
(66) Daugherty, R. G.; Wasowicz, T.; Gibney, B. R.; DeRose, V. J. *Inorg. Chem.* **2002**, *41*, 2623−2632.
(67) Harwell, D. E.; McMillan, J.; Knobler, C. B.; Hawthorne, M. F. *Inorg. Chem.* **1997**, *36*, 5951−5955.
(68) De Kerpel, J. O. A.; Ryde, U. *Proteins* **1999**, *36*, 157−174.
(69) Penfield, K. W.; Gewirth, A. A.; Solomon, E. I. *J. Am. Chem. Soc.* **1985**, *107*, 4519−4529.
(70) George, S. J.; Lowery, M. D.; Solomon, E. I.; Cramer, S. P. *J. Am. Chem. Soc.* **1993**, *115*, 2968−2969.

retention of a Cu^{I}-like state in oxidized blue copper sites was first proposed some time ago,[71] and contemporaneous SCF-X_α scattered wave calculations[69] verified by later copper L-edge XAS spectroscopy[70] showed that the singly occupied HOMO in oxidized plastocyanin includes only 41% Cu^{II}. That is, the effective oxidation state of this copper is not more than about $Cu^{1.4+}$. Other oxidized blue copper protein sites are most likely similar.[72]

Given this, it is inappropriate to ground an analysis of the geometric preference of copper within oxidized blue copper sites on the crystal structures of low MW copper complexes in which the effective copper valence is much more nearly 2+. If the valence of Cu^{I} increases by distinctly less than half following oxidation and if unconstrained Cu^{2+} is already preferentially D_{2d}-distorted, it should not be too surprising that a protein ligation site exists within which both metal states find a structural optimum in a pseudo-tetrahedral geometry.[38,73,74]

After questioning the rack-bonding hypothesis of the blue copper protein active site in terms of the structural preferences of unconstrained Cu^{II}, the complementary examination in terms the protein itself becomes incumbent. We thus next consider the rack-induced bonding hypothesis of blue copper proteins from a protein-thermodynamic perspective that has not heretofore received appropriate attention.

Rack Bonding from the Protein Perspective: The Marginal Stability of the Protein Fold. Proteins overall have a low thermodynamic stability against spontaneous unfolding, generally amounting to $\Delta G_{U\rightarrow N} \sim -(21-63)$ kJ mol^{-1},[75−77] where "U → N" represents the reversible unfolded-to-native transition. As a result of this low thermodynamic stability, native proteins dynamically populate a large number of conformational substates that are separated by relatively low thermodynamic barriers[78−80] and undergo occasional large conformational excursions.[79,81,82] Both azurin[83−85] and plastocyanin[86] equilibrate among such conformational substates. These motions are not consistent with a rigidly constrained protein fold and provide the context of the analyses developed below.

Folding Thermodynamics of Blue Copper Proteins: Local Strain and Global Structure. If the rack hypothesis is considered correct, then the strain energy residing in a nonoptimal geometry at a blue copper site of either oxidation state must be overcome by the secondary or tertiary structure of the protein. This question has been addressed by way of free-energy perturbation calculations on plastocyanin and nitrite reductase.[68] However, resistance by a protein of strain in a metal site should have thermodynamic consequences for the stability of the protein fold that are visible to experimental test.

In the folding of blue copper proteins, the global $\Delta G^{total}_{U\rightarrow N}$ must be negative. If the metal site in blue copper proteins is strained, then for these proteins $-\Delta G^{total}_{U\rightarrow N} = -\Delta G^{protein}_{U\rightarrow N} + \Delta G^{strain}_{U\rightarrow N}$, and $|\Delta G^{protein}_{U\rightarrow N}| > |\Delta G^{strain}_{U\rightarrow N}|$. The rack-bonding hypothesis says that the endergonic strain, $+\Delta G^{strain}_{U\rightarrow N}$, is produced at the metal site but only after the metal ion is bound. The energetic cost of imposing a nonoptimal metal geometry must then be compensated elsewhere in the protein by production of a local configuration that reaches a unique thermodynamic minimum *through the same folding process* that imposes thermodynamic strain at the metal site. That is, every folding trajectory must pass through a nexus in which the new appearance of endergonic strain at the metal site is compensated by the prior or simultaneous appearance of a compensating exergonic stability in the folding protein. This $|-\Delta G^{compensating}_{U\rightarrow N}|$ must be $\geq |+\Delta G^{strain}_{U\rightarrow N}|$, otherwise during folding there will be no net driving force to introduce local strain at the metal site and the protein will fold to a different structure representing a deeper global energy minimum in which the metal-site strain is relieved.

The $Cu-S_{Cys112}$ and $Cu-N_{His117}$ bonds remain intact in unfolded holoazurin, in each of the biological oxidation states.[87−90] Thus, the proposed $\Delta G^{strain}_{U\rightarrow N}$ should be present during refolding of the unfolded holoprotein, but absent during refolding of the unfolded apoprotein. If reversibly unfolded apo- and holocopper proteins each refold to the same native structure with the same suite of amino acid contacts, it is necessarily true that $|\Delta G^{apo}_{U\rightarrow N}| > |\Delta G^{holo}_{U\rightarrow N}|$ because $-\Delta G^{holo}_{U\rightarrow N}$ includes the endergonic rack-strain energy, $+\Delta G^{strain}_{U\rightarrow N}$, and $|\Delta G^{apo}_{U\rightarrow N}| - |\Delta G^{holo}_{U\rightarrow N}| = |\Delta G^{strain}_{U\rightarrow N}|$. More explicitly, given an invariant protein structure, the rack-bonding hypothesis predicts that $|-\Delta G^{apo}_{U\rightarrow N}| > |-\Delta G^{holo}_{U\rightarrow N}|$, because the $-\Delta G^{compensating}_{U\rightarrow N}$ that overcomes the $+\Delta G^{strain}_{U\rightarrow N}$ should make an unopposed appearance in the folding thermodynamics of the apoprotein.

(71) Frank, P.; Licht, A.; Tullius, T. D.; Hodgson, K. O.; Pecht, I. *J. Biol. Chem.* **1985**, *260*, 5518−5525.
(72) Olsson, M. H. M.; Ryde, U.; Roos, B. O.; Pierloot, K. *J. Biol. Inorg. Chem.* **1998**, *3*, 109−125.
(73) Ryde, U.; Olsson, M. H. M.; Pierloot, K.; Roos, B. O. *J. Mol. Biol.* **1996**, *261*, 586−596.
(74) Ryde, U.; Olsson, M. H. M. *Intl. J. Quantum Chem.* **2001**, *81*, 335−347.
(75) Pfeil, W. *Mol. Cell. Biochem.* **1981**, *40*, 3−28.
(76) Shortle, D.; Meeker, A. K. *Proteins: Struct. Funct. Genet.* **1986**, *1*, 81−89.
(77) Liu, L.; Yang, C.; Guo, Q. X. *Biophys. Chem.* **2000**, *84*, 239−251.
(78) Frauenfelder, H.; Sligar, S. G.; Wolynes, P. G. *Science* **1991**, *254*, 1598−1603.
(79) Vendruscolo, M.; Paci, E.; Dobson, C. M.; Martin Karplus, M. *J. Am. Chem. Soc.* **2003**, *125*, 15686−15687.
(80) Fenimore, P. W.; Frauenfelder, H.; McMahon, B. H.; Young, R. D. *Proc. Natl. Acad. Sci. U.S.A.* **2004**, *101*, 14408−14413.
(81) Tang, K. E. S.; Dill, K. A. *Int. J. Quantum Chem.* **1999**, *75*, 147−164.
(82) Wand, A. J. *Nat. Struct. Biol.* **2001**, *8*, 926−931.
(83) Ehrenstein, D.; Nienhaus, G. U. *Proc. Natl. Acad. Sci. U.S.A.* **1992**, *89*, 9681−9685.
(84) Ehrenstein, D.; Filiaci, M.; Scharf, B.; Engelhard, M.; Steinbach, P. J.; Nienhaus, G. U. *Biochemistry* **1995**, 12170−12177.
(85) Korzhnev, D. M.; Karlsson, B. G.; Orekhov, V. Y.; Billeter, M. *Protein Sci.* **2003**, *12*, 56−65.
(86) Bertini, I.; Bryant, D. A.; Cuirli, S.; Dikyi, A.; Fernández, C. O.; Luchinat, C.; Safrov, N.; Vila, A. J.; Zhao, J. *J. Biol. Chem.* **2001**, *276*.
(87) Leckner, J.; Wittung, P.; Bonander, N.; Karlsson, B. G.; Malmström, B. G. *J. Biol. Inorg. Chem.* **1997**, *2*, 368−371.
(88) Wittung-Stafshede, P.; Hill, M. G.; Gomez, E.; DiBilio, A. J.; Karlsson, B. G.; Leckner, J.; Winkler, J. R.; Gray, H. B.; Malmström, B. G. *J. Biol. Inorg. Chem.* **1998**, *4*, 367−370.
(89) DeBeer, S.; Wittung-Stafshede, P.; Leckner, J.; Karlsson, G.; Winkler, J. R.; Gray, H. B.; Malmström, B. G.; Solomon, E. I.; Hedman, B.; Hodgson, K. O. *Inorg. Chim. Acta* **2000**, *297*, 278−282.
(90) Pozdnyakova, I.; Guidry, J.; Wittung-Stafshede, P. *J. Biol. Inorg. Chem.* **2001**, *6*, 182−188.

Reversibly denatured apoazurin[91,92] and apoplastocyanin[93] do indeed refold to the fully native conformation, and the native apoproteins have the same crystal structures as the respective holoproteins both globally and in the metal-binding region[94−96] (see below). This invariant fold shows that the apo- and holoproteins should indeed have the same suite of amino acid contacts. Thus, the above thermodynamic considerations apply and $|-\Delta G^{apo}_{U\rightarrow N}|$ should be larger than $|-\Delta G^{holo}_{U\rightarrow N}|$.

However, in either oxidation state, the refolding free energy of holoazurin (Cu^{II}, ~ -52 kJ mol^{-1}; Cu^{I} ~ -40 kJ mol^{-1}) is much greater than the refolding free energy of apoazurin (~ -28 kJ mol^{-1}),[87,91,92,97−99] despite the fact that all three forms fold to the identical global conformation. Thus, copper ion coordination in either oxidation state increases rather than decreases the stability of the native fold of azurin. The same is true with holoplastocyanin, at least in the oxidized form.[93] An early calorimetric study intimated the same result,[97,100] showing that holoazurin is more stable than apoazurin. These results are the reverse of what is predicted by rack bonding and disconfirm the hypothesis both in the original Cu^{II} form and in the later Cu^{I} form.

Structural Thermodynamics of Apo- versus Holoprotein Refolding. In light of the identical structure of apo- and holoproteins, the entire $\Delta G_{U\rightarrow N}$ for apoazurin, which is ~ -28 kJ mol^{-1} [91,92,99] and which must include the entire $-\Delta G^{compensating}_{U\rightarrow N}$ predicted to be present by the rack hypothesis, is wholly insufficient to overcome the $\sim$70 kJ mol^{-1} of positive rack-strain energy originally proposed to be additionally present in the oxidized metal site of blue copper proteins.[16] This disparity predicts that unfolded Cu^{II} holoazurin should not spontaneously refold into the native state at all, because $\Delta G_{net} \sim +42$ kJ mol^{-1} for this process. The rack-bonding hypothesis thus predicts that, if reversibly unfolded Cu^{II} holoazurin does refold, it should produce a non-native conformation for which $\Delta G_{folding}$ is negative.

Likewise, the $\sim +29$ kJ mol^{-1} rack-strain energy more recently proposed to enforce the geometry of the reduced, Cu^{I}, blue copper site[60,62] is about equal in magnitude to the ~ -28 kJ mol^{-1} $\Delta G_{U\rightarrow N}$ for apoazurin. This Cu^{I} form of the rack-bonding hypothesis then predicts that reversibly unfolded reduced holoazurin should advance only to a 1:1 equilibrium with its folded state because for this process $\Delta G_{U\rightarrow N} \sim 0$ kJ mol^{-1} ($K_{U\rightarrow N} = 1$, when $\Delta G_{U\rightarrow N} = 0$ kJ mol^{-1}). However, reversibly unfolded azurin in both oxidized and reduced forms fully refolds to the native protein state.[87,92,98] This must mean that the predicted endergonic rack strain does not appear in either folding process. Each of the rack-model predictions is thus again contradicted by the experiment.

Copper Addition as an Insertion Mutation. The above deductions regarding equilibrium between folded and unfolded holo-blue copper proteins are given experimental credibility by reference to single amino acid insertions into native staphylococcal nuclease,[101] which exhibits a native folding free energy $\Delta G_{U\rightarrow N} = -23.5$ kJ mol^{-1}. Amino acid insertion mutants destabilized the folded state by 6.1−33.5 kJ mol^{-1}, averaging 23.9 kJ mol^{-1} for insertions into α helices and 24.3 kJ mol^{-1} for insertions into β sheets. The destabilization energy of several of the insertion mutants produced a $\Delta G_{U\rightarrow N} \sim 0$ kJ mol^{-1} and thus $K_{U\rightarrow N} \sim 1$. These proteins existed in a solution equilibrium of $\sim$1:1 folded/unfolded states.

Introduction of Cu^{I} or Cu^{II} into apoazurin is analogous to preparation of an insertion mutant, because the metal ion is a structural inclusion that produces an additional thermodynamic contribution to the native protein fold. After insertion of Cu^{II}, the newly imposed rack-strain $\Delta G_{strain} = \sim +70$ kJ mol^{-1} would overcome the $-\Delta G_{U\rightarrow N} = \sim -28$ kJ mol^{-1} of stability for apoazurin, forcing the protein to spontaneously unfold. Likewise, if Cu^{I} holoazurin is strain-free, then oxidation will introduce the rack strain and the protein should spontaneously unfold.

Correspondingly, if the Cu^{I} form of the rack-induced bonding hypothesis is entertained, then the new $\Delta G_{strain} \sim +29$ kJ mol^{-1} of rack strain following insertion of Cu^{I} into apoazurin should just erase the $\Delta G \sim -28$ kJ mol^{-1} of apoprotein stabilizing free energy and the protein should spontaneously enter a $\sim$1:1 equilibrium with the unfolded state. Alternatively, if oxidized azurin is strain-free, then reduction should induce the identical $\sim$1:1 folded/unfolded equilibrium.

Clearly, none of these rack-derived predictions is borne out in fact. The protein fold of azurin is robust both to the addition of copper in either oxidation state and to redox cycling, again contradicting explicit predictions of the protein rack hypothesis.

View of the Cu^{II} Rack-Model from Semisynthetic Blue Copper Proteins. Semisynthetic blue copper protein sites have been prepared within foreign proteins for which no selective evolutionary gradient toward an impositional rack could reasonably have occurred. These include hexameric insulin,[102−104] liver alcohol dehydrogenase (LADH),[105−110] and copper−zinc superoxide dismutase.[111]

(91) Mei, G.; Di Venere, A.; Campeggi, F. M.; Gilardi, G.; Rosato, N.; De Matteis, F.; Finazzi-Agro, A. *Eur. J. Biochem.* **1999**, *265*, 619−626.
(92) Pozdnyakova, I.; Wittung-Stafshede, P. *Biochemistry* **2001**, *40*, 13728−13733.
(93) Koide, S.; Dyson, H. J.; Wright, P. E. *Biochemistry* **1993**, *32*, 12299−13310.
(94) Nar, H.; A., M.; Huber, R.; van de Kamp, M.; Canters, G. W. *FEBS Lett.* **1992**, *306*, 119−124.
(95) Shepard, W. E. B.; Kingston, R. L.; Anderson, B. F.; Baker, E. N. *Acta Crystallogr., Sect. D* **1993**, *49*, 331−343.
(96) Garrett, T. P. J.; Clingeleffer, D. J.; Guss, J. M.; Rogers, S. J.; Freeman, H. C. *J. Biol. Chem.* **1984**, *259*, 2822−2825.
(97) Engeseth, H. R.; McMillin, D. R. *Biochemistry* **1986**, *25*, 2448−2455.
(98) Winkler, J. R.; Wittung-Stafshede, P.; Keckner, J.; Malmström, B. G.; Gray, H. B. *Proc. Natl. Acad. Sci. U.S.A.* **1997**, *94*, 4246−4249.
(99) Hansen, J. E.; McBrayer, M. K.; Robbins, M.; Suh, Y. *Cell Biochem. Biophys.* **2002**, *36*, 19−40.
(100) McMillin, D. R.; Engeseth, H. R. *The Blue Copper Binding Site: From the Rack or Tailor Made?*; in *Biological and Inorganic Copper Chemistry*; Karlin, K. D., Zubieta, J., Eds.; Adenine: Guilderland, NY, 1986; pp 1−10.
(101) Sondek, J.; Shortle, D. *Proteins: Struct. Funct. Genet.* **1990**, *7*, 299−305.
(102) Brader, M. L.; Dunn, M. F. *J. Am. Chem. Soc.* **1990**, *112*, 4585−4587.
(103) Brader, M. L.; Borchardt, D.; Dunn, M. F. *J. Am. Chem. Soc.* **1992**, *114*.

The insulin blue copper mimic follows an allosteric conformational change between the T_6 and R_6 insulin hexamers;[112] in that, only R_6 insulin can bind two metal ions within two identical tetrahedral sites that include three histidine imidazole ligands, plus one replaceable water ligand derived from the solvent.[103,104,113] The dominant hexameric form is T_6 insulin,[113,114] but titration of $T_6Co^{II}_2$ insulin with *m*-cresol[115] induces R_6(*m*-cresol)$_6Co^{II}_2$ insulin, driven by $\Delta G \sim -33 \pm 1$ kJ mol^{-1} of *m*-cresol binding free energy. In contrast, only addition of both phenol and strong copper ligands will induce a $T_6 \rightarrow R_6$ allosteric transition in $T_6Cu^{II}_2$ insulin.[104] Thus, excess phenol plus the thiolate ligand *p*-CH_3-PhS$^-$ induces two tetrahedral $R_6(\text{phenol})_6[Cu(N_{His})_3(S\text{Ph-}p\text{-}CH_3)]_2$ insulin sites that reproduce the entire typifying spectroscopic signature of blue copper proteins.[102,104,113] Tellingly, the fact that the $T_6(\text{phenol})_6Cu^{II}_2$ to $R_6(\text{phenol})_6Cu^{II}_2$ transition is driven only by the addition of a strong fourth ligand means that a rigid protein rack does not impose the tetrahedral geometry of the semisynthetic blue site. Instead, the drive to two blue tetrahedral $[Cu^{II}(N_{His})_3(S\text{Ph-}p\text{-}CH_3)]$ sites induces the $T_6 \rightarrow R_6$ conformational transition. This result contradicts that oxidized blue protein sites require an endergonic protein rack.

LADH provides a Cu^{II}-binding site consisting of Cys46, Cys174, His67, and a water molecule,[116] which produces spectroscopy resembling that of blue copper proteins.[105−108,117] Added pyrazole binds near the metal site of Cu^{II}-LADH and changes the EPR spectrum from that of rhombic blue copper to axial type-2-like copper, indicating flexibility in the metal site.[105,110] In native Zn^{II} LADH, the analogous pyrazole binding[118] yields an upper limit estimate of 12 kJ mol^{-1} for the type-1 to type-2 transformation of Cu^{II} LADH. Thus, any strain energy in the Cu^{II}-LADH blue site must be $< \sim$12 kJ mol^{-1}, otherwise this semisynthetic blue site would spontaneously transition to a type-2 site. A total of 12 kJ mol^{-1} of free energy is much less than the $\sim$70 kJ mol^{-1} of rack-bond energy predicted to be necessary to impose the supposed unfavorable geometry of the oxidized blue copper site.

The existence of these semisynthetic blue sites in the absence of any special evolutionary design and any evident rack energy do not support a conclusion of constraint by necessity.

Flexibility in the Metal-Binding Site of Blue Copper Proteins. Uptake of a water molecule into the empty copper site of apo-*Pseudomonas aeruginosa* azurin is accompanied by 2.2 Å motions of the copper ligands His46 and His117, along with smaller motions of other surrounding side chains, all in a dynamic water-exchange solution equilibrium.[94]

In the His117Gly mutant of holoazurin, the 116−120 loop was found to undergo significant thermal motions, as well as movements to accommodate the steric needs of a variety of exogenous copper ligands,[119] despite the fact that the mutation should not have affected the hydrogen-bonding network proposed to be part of the stiffening rack for the His117 ligand.[56]

In the magnificent crystallographic study of Cu^I poplar plastocyanin, the acid-induced tetrahedral−trigonal transformation of the metal site showed the His87 imidazole ligand to protonate, dissociate from Cu^I, rotate 180°, and shift 0.5 Å, while the Cu^I−SMet92 bond length decreased from 2.9 to 2.5 Å. These motions were not accompanied by any significant global protein rearrangements and were interpreted as part of a dynamic pH-dependent solution equilibrium.[120] An analogous shift of the Met121 sulfur ligand was noted on reduction of the His117Gly mutant of azurin.[119] These motions do not support the idea that the Cu^I-S_{Met} bond length is restricted to 2.9 Å by the protein.[57−59] Likewise, major rearrangements of the amino acid side chains of the metal-binding site in Met121His *Alcaligenes denitrificans* azurin were found to follow protonation of the new His121 ligand. This was interpreted to mean that, "the metal ... codetermines the structure of its own site".[121]

These motions of three of the four ligand side chains in blue copper proteins show that the hydrogen bonds found in the region of the blue copper site of azurin[56] apparently have little, if anything, to do with enforcing a rigid ligand geometry. They comport with calculational predictions[68,74] supporting the same conclusion and are consistent with the protein flexibility and structural excursions that stem from the low thermodynamic stability of folded proteins as outlined above.

To summarize the points of this analysis: Unconstrained aqua Cu^{II} ion and other low MW Cu^{II} complexes spontaneously support an irregular D_{2d}-distorted equatorial ligand geometry. Oxidized blue copper proteins contain $Cu^{\sim 1.4+}$ and

(104) Brader, M. L.; Borchardt, D.; Dunn, M. F. *Biochemistry* **1992**, *31*, 4691−4696.
(105) Maret, W.; Dietrich, H.; Ruf, H.-H.; Zeppezauer, M. *J. Inorg. Biochem.* **1980**, *12*, 241−252.
(106) Maret, W.; Zeppezauer, M.; Desideri, A.; Morpurgo, L.; Rotilio, G. *FEBS Lett.* **1981**, *136*, 72−74.
(107) Maret, W.; Zeppezauer, M.; Sanders-Loehr, J.; Loehr, T. M. *Biochemistry* **1983**, *22*, 3202−3206.
(108) Maret, W.; Shiemke, A. W.; Wheeler, A. K.; Loehr, T. M.; Sanders-Loehr, J. *J. Am. Chem. Soc.* **1986**, *108*, 6351−6359.
(109) Maret, W.; Zeppezauer, M.; Desideri, A.; Morpurgo, L.; Rotilio, G. *Biochim. Biophys. Acta* **2003**, *743*, 200−206.
(110) Al-Karadaghi, S.; Cedergren-Zeppezauer, E. S.; Dauter, Z.; Wilson, K. S. *Acta Crystallogr., Sect. D* **1995**, *51*, 805−813.
(111) Lu, Y.; Lacroix, L. B.; Lowery, M. D.; Solomon, E. I.; Bender, C. J.; Peisach, J.; Roe, J. A.; Gralla, E. B.; Valentine, J. S. *J. Am. Chem. Soc.* **1993**, *115*, 5907−5918.
(112) Bloom, C. R.; Choi, W. E.; Brzovic, P. S.; Ha, J. J.; Huang, S.-T.; Kaarsholm, N. C.; Dunn, M. F. *J. Mol. Biol.* **1995**, *245*, 324−330.
(113) Brader, M. L.; Kaarsholm, N. C.; Lee, R. W.-K.; Dunn, M. F. *Biochemistry* **1991**, *30*, 6636−6645.
(114) Choi, W. E.; Borchardt, D.; Kaarsholm, N. C.; Brzovic, P. S.; Dunn, M. F. *Proteins* **1996**, *26*, 377−390.
(115) Choi, W. E.; Brader, M. L.; Aguilar, V.; Kaarsholm, N. C.; Dunn, M. F. *Biochemistry* **1993**, *32*, 11638−11645.
(116) Farrar, J. A.; Formicka, G.; Zeppezauer, M.; Thomson, A. J. *Biochem. J.* **1996**, *317*, 447−456.
(117) Eklund, H.; Samama, J.-P.; Wallén, L. *Biochemistry* **1982**, *21*, 4858−4866.
(118) Andersson, P.; Kvassman, J.; Lindström, A.; Oldén, B.; Pettersson, G. *Eur. J. Biochem.* **1981**, *114*, 549−554.
(119) Jeuken, L. J. C.; Ubbink, M.; Bitter, J. H.; van Vliet, P.; Meyer-Klaucke, W.; Canters, G. W. *J. Mol. Biol.* **2000**, *299*, 737−755.
(120) Guss, J. M.; Harrowell, P. R.; Murata, M.; Norris, V. A.; Freeman, H. C. *J. Mol. Biol.* **1986**, *192*, 361−387.
(121) Messerschmidt, A.; Prade, L.; Kroes, S. J.; Sanders-Loehr, J.; Huber, R.; Canters, G. W. *Proc. Natl. Acad. Sci. U.S.A.* **1998**, *95*.

not Cu^{II}. The known low thermodynamic stability of native-folded proteins cannot support any significant endergonic rack strain. The thermodynamics attending the rack-bonding hypotheses predict that either oxidized or reduced blue copper proteins should spontaneously denature. Semisynthetic blue copper proteins show no evidence of a stabilizing rack. The amino acid ligands of the blue copper site can exhibit large translational excursions. These multiple independent experimental contradictions of explicit predictions of the rack-bonding hypotheses for Cu^{II} and Cu^{I} blue copper proteins permit a general conclusion: the rack-bonding hypothesis is experimentally unjustifiable.

In light of this, one is left to explain the unusual structure and bonding of the blue copper protein metal site in terms of the physical bioinorganic chemistry of the site itself, without any recourse to a protein rack. This appears quite feasible. First, the protein metal-binding cavity is enclosed enough to prevent decomposition of the active site through oxido-reductive dissociation of the $Cu^{II}-$thiolate bond.[73,98,119,122] Second, the active-site imidazole and cysteinate ligands bind near the equatorial plane of Cu^{II}, where the calculational results reported here and elsewhere[38,58,59,69,72,123] show that covalent interaction with the singly occupied metal 3d $_{x^2-y^2}$ orbital is greatest. The high covalence of the $[Cu-S_{Cys}]^{1+}$ bond reduces the valence state of copper to much less than 2+ in the oxidized blue copper protein site.[57,60,62,68−72] The results reported here that the unconstrained, nearly fully divalent $[Cu(H_2O)_5]^{2+}$ ion supports D_{2d}-distorted equatorial ligands and is energetically proximate to fully four-coordinate D_{2d}-distorted $[Cu(H_2O)_4]^{2+}$ show that the preferred geometry of unconstrained Cu^{II} is already close to a structure supported by Cu^{I}. The small valence change of copper during a redox cycle, i.e., 1+ ⇌ ∼1.4+, almost fully harmonizes the structural requirements of copper in the two protein oxidation states,[73] thus minimizing the Franck−Condon redox barrier. Third, the electrostatic field and lipotropism of the protein environment and, fourth, ligand perturbations, such as protonation,[124] tune the redox potential of the active site.[57,60,62,73,125]

Any residual structural strain at the copper site,[60−62] driven by the formation of strong metal−ligand bonds, should be small and compensated primarily by adjustments within the immediate carbon backbone of the ligands, for example, in the possible production of a countervailing gauche strain[126] directed along the carbon skeleton. Whatever residual strain that might appear in the copper site is not detectible in the secondary or tertiary structure of the protein as noted above.

This analysis would be falsified if a detailed examination of the secondary and/or tertiary structures of the crystallized reduced or oxidized blue copper holoproteins revealed heretofore unseen stabilizing interactions not present in the apoproteins. These interactions should more than compensate for any thermodynamic rack strain newly imposed on the apoprotein by metalation of the active site, in a manner that preserves the known increased folding stability of the holoproteins. However, no such stabilizing differences have been thus far reported from the high-resolution structures of apo- and holoplastocyanin[96,120,127] or azurin.[94,95]

In summary, the geometrical invariance at copper during redox, characteristic of blue copper protein sites, can be better described as the result of an evolutionary selection to match the irregular geometry spontaneously sustainable by copper in both biological oxidation states with a ligand array evolved to provide high covalence near the equatorial plane where Cu^{II} localizes such bonding, thus minimizing the redox-induced valence change *at copper*. The state of *entasis*[26] is then approached by persuasion rather than by coercion, as noted previously.[71]

Finally, the new results reported here show that aqua Cu^{II} departs radically from the general view that transition-metal ions are octahedrally six-coordinate in water solution. Arguments for the preferred ligation arrangement of unconstrained metal ions apparently should not be couched in the geometries found in crystal structures alone.

Acknowledgment. P. F. thanks Prof. Thomas Loehr for providing several helpful citations and Prof. Sebastian Doniach for his critical and constructive interest in this work. This work was supported by Grant NIH RR-01209 (to K. O. H.) and Grant NSF EpSCOR and computational time from the Center for Computational Biology, MSU (to R. K. S.). M. B. acknowledges financial support from SSRL during a 1-month stay as a visiting scientist. XAS data were measured at the EMBL spectrometer at HASYLAB, Hamburg, Germany. The SSRL Structural Molecular Biology Program is supported by the National Institutes of Health, National Center for Research Resources, Biomedical Technology Program and by the Department of Energy, Office of Biological and Environmental Research.

Supporting Information Available: Cartesian coordinates and Supplemental Figure 1. This material is available free of charge via the Internet at http://pubs.acs.org.

IC0400639

(122) Dong, S. L.; Ybe, J. A.; Hecht, M. H.; Spiro, T. G. *Biochemistry* **1999**, *38*, 3379−3385.
(123) Olsson, M. H. M.; Ryde, U. *J. Biol. Inorg. Chem.* **1999**, *4*, 654−663.
(124) Glaser, T.; Hedman, B.; Hodgson, K. O.; Solomon, E. I. *Acc. Chem. Res.* **2000**, *33*, 859−868.
(125) Berry, S. M.; Ralle, M.; Low, D. W.; Blackburn, N. J.; Lu, Y. *J. Am. Chem. Soc.* **2003**, *125*, 8760−8768.
(126) Smith, M. B.; March, J. *March's Advanced Organic Chemistry: Reactions, Mechanisms, and Structure*; 5th ed.; John Wiley and Sons: New York, 2001; p 170.
(127) Garrett, T. P. J.; Clingeleffer, D. J.; Guss, J. M.; Rogers, S. J.; Freeman, H. C. *J. Biol. Chem.* **1984**, *259*, 2822−2825.